AD-A129 436 AEROSOL SPECTRA OBSERVED IN MARINE STRATUS CLOUDS ANALYSIS OF AIRBORNE MU..(U) NAVAL OCEAN SYSTEMS CENTER SAN DIEGO CA V R NOONKESTER 13 APR 83 NOSC/TD-586 1/1

UNCLASSIFIED F/G 4/2 NL

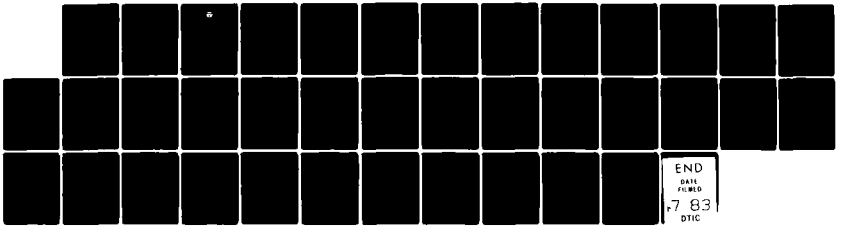

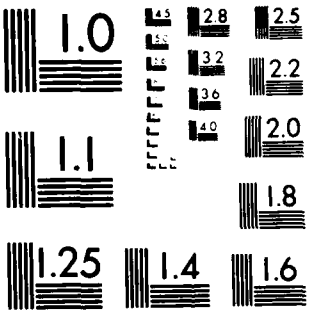

NOSC TD 586

NOSC TD 586

Technical Document 586

AEROSOL SPECTRA OBSERVED IN MARINE STRATUS CLOUDS

Analysis of airborne multilevel measurements taken 130 km SW of San Diego

VR Noonkester

13 April 1983

Period of work:
August 1981–April 1983

Prepared for
Naval Air Systems Command
Code 333

Approved for public release; distribution unlimited

NOSC
NAVAL OCEAN SYSTEMS CENTER
San Diego, California 92152

NAVAL OCEAN SYSTEMS CENTER, SAN DIEGO, CA 92152

AN ACTIVITY OF THE NAVAL MATERIAL COMMAND

JM PATTON, CAPT, USN
Commander

HL BLOOD
Technical Director

ADMINISTRATIVE INFORMATION

Work was performed under program element 61153N, project WR03302 (NOSC 532-MP04) by a member of the Tropospheric Branch (Code 5325) for Naval Air Systems Command, Code 333. This document covers work from August 1981 to April 1983 and was approved for publication 13 April 1983.

The author is indebted to DR Jensen, who diligently acquired excellent data and provided insight into making these measurements through use of the NOSC aircraft system, and to BL Thomason, who processed the data with great care.

Released by
JH Richter, Head
Ocean and Atmospheric
Sciences Division

Under authority of
JD Hightower, Head
Environmental Sciences
Department

CONVERSION TO SI METRIC

To convert from	to	Multipy by
degrees (°), angle	rad	$\sim 1.75 \times 10^{-2}$
millibars (mb)	Pa	10^{2}
miles per hour (mph)	m/s	$\sim 4.47 \times 10^{-1}$

UNCLASSIFIED

SECURITY CLASSIFICATION OF THIS PAGE (When Data Entered)

REPORT DOCUMENTATION PAGE		READ INSTRUCTIONS BEFORE COMPLETING FORM
1. REPORT NUMBER NOSC Technical Document 586 (TD 586)	2. GOVT ACCESSION NO. AD-A129 436	3. RECIPIENT'S CATALOG NUMBER
4. TITLE (and Subtitle) AEROSOL SPECTRA OBSERVED IN MARINE STRATUS CLOUDS Analysis of airborne multilevel measurements taken 130 km SW of San Diego		5. TYPE OF REPORT & PERIOD COVERED Interim August 1981–April 1983 6. PERFORMING ORG. REPORT NUMBER
7. AUTHOR(s) VR Noonkester		8. CONTRACT OR GRANT NUMBER(s)
9. PERFORMING ORGANIZATION NAME AND ADDRESS Naval Ocean Systems Center San Diego CA 92152		10. PROGRAM ELEMENT, PROJECT, TASK AREA & WORK UNIT NUMBERS PE 61153N Proj WR03302 (NOSC 532-MP04)
11. CONTROLLING OFFICE NAME AND ADDRESS Naval Air Systems Command, Code 333 Washington DC 20361		12. REPORT DATE 13 April 1983 13. NUMBER OF PAGES 34
14. MONITORING AGENCY NAME & ADDRESS(if different from Controlling Office)		15. SECURITY CLASS. (of this report) Unclassified 15a. DECLASSIFICATION DOWNGRADING SCHEDULE

16. DISTRIBUTION STATEMENT (of this Report)

Approved for public release; distribution unlimited

17. DISTRIBUTION STATEMENT (of the abstract entered in Block 20, if different from Report)

18. SUPPLEMENTARY NOTES

19. KEY WORDS (Continue on reverse side if necessary and identify by block number)

Aerosols
Aerosol size spectra
Marine stratus cloud layers

20. ABSTRACT (Continue on reverse side if necessary and identify by block number)

Airborne measurements of the aerosol size spectra, n(r), for radii between 0.23 and 150 μm were made at about 14 levels in stratus layers 130 km SW of San Diego during May and August 1981. Both marine and continental air masses were represented. Four parameters were derived from 15 n(r)s observed along each level for a distance of 6.44 km and from the average n(r) over the entire run. Profiles of the four parameters were constructed as a function of the distance from the cloud base. Profiles on the marine and continental days differed: the continental day contained many more small aerosols.

DD FORM 1 JAN 73 1473 EDITION OF 1 NOV 65 IS OBSOLETE

S N 0102-LF-014-6601

UNCLASSIFIED

SECURITY CLASSIFICATION OF THIS PAGE (When Data Entered)

SUMMARY

Airborne measurements of the aerosol spectra, n(r) (r is radius), for 0.23 μm $\leq$ r $\leq$ 150 μm were made at about 14 levels in stratus layers 130 km SW of San Diego during May and August 1981. All May days were found to be associated with marine air masses; all August days, with continental air masses. One day in May and one day in August were selected as representative of the marine and continental air mass seasons, respectively. Four parameters were derived from 15 n(r)s observed along each level for a distance of 6.44 km and from the average n(r) over the entire run.

Profiles of the four parameters were constructed as a function of the distance from the cloud base, defined to be the level at which the liquid water content is 0.02 g/m^3. Profiles on the marine and continental days differed: the continental day contained many more small aerosols. The profile of the liquid water content was closely examined in the region from 250 m below to 250 m above the cloud base.

The average horizontal scale size of the four parameters was estimated to be 3.7 km in and near the clouds. The horizontal variability of an aerosol parameter was defined to be the ratio of its standard deviation to its average at any level. Variability was highest near the cloud base and top and lowest near midcloud, suggesting enhancement of horizontal variation by vertical mixing across the saturation levels. The correlation coefficients between pairs of aerosol parameters along each level show no consistent vertical pattern except that the number of aerosols and the liquid water content are positively correlated at all levels. These correlations do not support inhomogeneous mixing.

The apparent horizontal variability created by an inadequate sampling volume by the aerosol spectrometers was examined. The horizontal sampling distances required to obtain a reliable average of each aerosol parameter were also estimated.

CONTENTS

1. INTRODUCTION

Vertical and temporal variations of the liquid-water aerosol spectrum, n(r) (where r is aerosol radius), in stratus-cloud layers over oceans are not well known. They continue to receive attention because persistent and extensive marine stratus-cloud decks appreciably influence the atmospheric radiation balance. Specification of n(r) in marine stratus clouds requires detailed knowledge of the turbulent and radiative properties of the mixed boundary layer (Schubert et al, 1979; Deardorff, 1980; Roach et al, 1982; Brost et al, 1982a, 1982b) and of the associated effects of turbulent mixing on n(r) (Baker et al, 1980; Telford and Chai, 1980). The number and chemical nature of both the condensation nuclei (generally controlled by the air mass source) and the sea-spray aerosols (regulated partly by surface wind speed) are also important in moderating the total number of aerosols, N, and the shape of n(r) in the mixed layer (Fitzgerald, 1974).

Detailed airborne observations of n(r) were made at many levels in marine stratus layers 110-150 km southwest of San Diego, California (fig 1), in May and August 1981. May and August aerosol data appeared to characterize marine and continental air masses, respectively. This document presents and compares aerosol data for a representative day in May and and one in August. Differences and similarities in the vertical and horizontal variations in parameters derived from n(r) were examined. The differences are concluded to be caused by contrasting air mass sources, and some evidence is presented to suggest that similarities are produced by similar turbulent mixing conditions.

2. SENSORS

Measurements of elevation, z, and aerosol spectra, n(r), were made aboard a twin-engine Piper Navajo flying at 54 m/s. Elevation, z, was measured by a radar (Bonzar Inc, model Mark-10X) and a pressure altimeter (Rosemount, model 542K). Above 40 m, the expected error in z by the pressure altimeter is much less than that of the radar altimeter. To compensate for any atmospheric pressure change between the airport and the measurement region, the altitude of the pressure altimeter was set prior to making measurements to the altitude

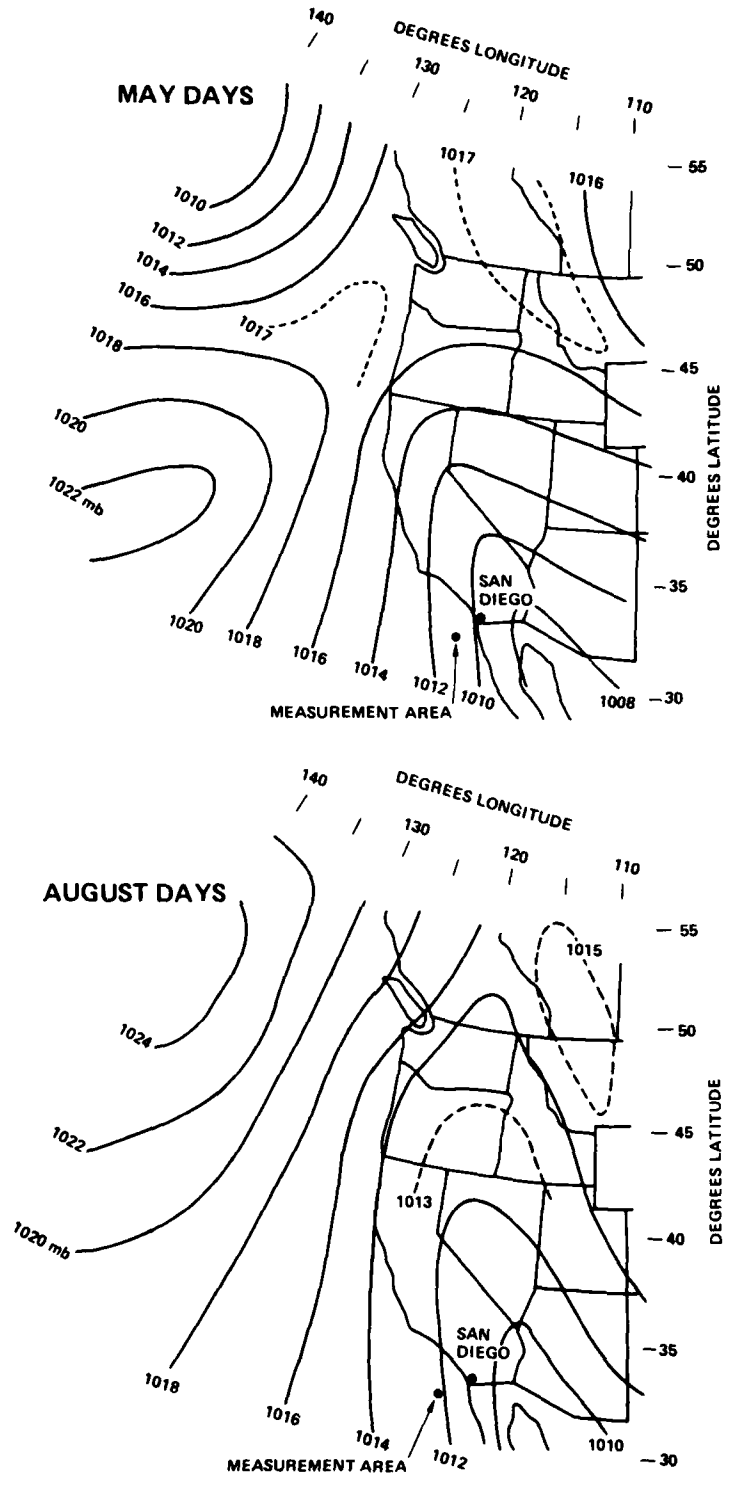

Figure 1. Representative surface pressure patterns for measurement days in May and August 1981. The measurement area location, near San Diego, is shown. The pressure patterns indicate a probable continental air mass present in the measurement area in August, a probable marine air mass in May.

given by the radar altimeter along a low-level horizontal flight. All subsequent elevations were taken from the pressure altimeter. Elevation and n(r) were sampled for 2 minutes along constant-level runs at 13 to 16 levels in stratus layers. Below 700 m, elevations—measured every 5 s—were accurate to about ±2-3 m. The minimum and maximum standard deviations of z along the 2-min horizontal measurement runs (6.44 km) were 1.6 and 8.9 m, respectively, and the average standard deviation was 4.7 m.

Two types of aerosol spectrometer probes, manufactured by Particle Measuring System Inc, were used to obtain an n(r) every 8 s (429 m). This provided 15 n(r)s, each representing 429 m, along each 2-min run. Probe ASSP-100 measured n(r)s in 32 radius bands in the range 0.23 to 14.7 μm, and probe OAP-200 measured n(r)s in 15 radius bands in the range 14.2 to 150 μm. All particles are processed by the probes as spherical droplets having a refractive index of pure water. Some improper size identifications are inherent in the ASSP-100 at small aerosol radii. Both probes were calibrated periodically.

No other measurements were available to provide checks on the reliability of the aerosol probes. A comparison of n(r) measured by several colocated PMS spectrometers for a 9-day period in May 1979 revealed variations in n(r) by factors of 10 for all radii (Jensen et al, 1983). Extinction coefficients for wavelengths from the visible to IR, calculated from these n(r)s, differed by factors of 2 to 3. Although the n(r)s have unknown absolute accuracy, their relative changes during a daily measurement period and between the May and August measurements are considered real.

3. MEASUREMENT PROCEDURE

A NW wind was observed at the coast on each measurement day in both May and August. Accordingly, the measurement region shown in figure 1 was chosen to avoid areas likely to be downwind of the coastal islands or of the California coast. Southwesterly flights were made from San Diego at 1 km altitude to find a region of extended homogeneous stratus clouds as viewed from above. After a measurement region was selected, a slow, slant-path descent was made through the stratus clouds to estimate the elevation of the cloud top z_t and cloud base z_c. A horizontal flight was made near the surface

of the ocean to set the elevation of the pressure altimeter to that of the radar altimeter and to estimate the surface wind direction by visual inspection of the water surface. There followed a series of 2-min horizontal runs at about the following elevations:

z_o (lowest safe elevation)

$z_c/5$

$z_c/2$

z_c - 80 m

z_c - 60 m

z_c - 40 m

z_c - 20 m

z_c

z_c + 20 m

z_c + 40 m

$(z_c + z_t)/2$

z_t - 40 m

z_t

z_t + 40 m

Horizontal flights were made at other levels when appropriate. To establish z_t, the pilot attempted to fly in the small cloud-top billows about 50 percent of the time. The direction of each run was 180° from that of the previous run. Accurate navigation aids were used to confine the measurement region essentially to a vertical plane extending about 8 km in the direction of the surface wind. Because the increase in the visibility near the "cloud bases" (as defined in section 4) was gradual along the descent, a definite z_c could not be established. Therefore z_c was estimated, and this estimation was used to establish the run elevations. Cloud tops could be estimated to be within ±10 m during the descent. If z_t changed more than ±30 m between the time of the descent and the horizontal run at z_t (~1 h time lapse), the stratus layer was considered to be nonstationary and the data were not used.

Measurements on 14, 28, and 29 May 1981 and on 11, 13, 14, 17, and 18 August 1982 were accepted as representing horizontally homogeneous and temporally unchanging marine stratus layers. The data for 29 May and 18 August were chosen for presentation here as characteristic of dissimilar air masses, subsequently concluded to be marine and continental air masses respectively. These days are hereinafter identified as M29 and A18. The horizontal runs were made from 0610 to 0654 PST on M29 and from 0814 to 0904 PST on A18. Neither solar heating of the stratus layer nor sea-breeze circulations should have had a significant effect on the stratus layer at these early morning hours during the short measurement periods. Early morning large-scale visual images by satellite verified the presence of an extensive uniform stratus deck over the ocean surrounding the measurement region.

4. PARAMETERS DERIVED FROM n(r)

The following parameters were derived from the aerosol spectrum, n(r).†

Total number of particles: $N \text{ (in cm}^{-3}) = \int n(r)\, dr$ (1)

Mean aerosol radius: $\bar{r} \text{ (in } \mu m) = \frac{1}{N} \int r\, n(r)\, dr$ (2)

Total cross-sectional area: $A \text{ (in cm}^2\text{m}^{-3}) = \pi \int r^2\, n(r)\, dr$ (3)

Total liquid water content: $w \text{ (in gm}^{-3}) = \frac{4}{3}\pi D \int r^3\, n(r)\, dr$ (4)

(where D = density of water, in g/cm^3)

Variance of r: $\sigma_r^2 \text{ (in } \mu m^2) = \frac{1}{N} \int (r - \bar{r})^2\, n(r)\, dr$ (5)

All integrations were performed numerically over the range $0.23\ \mu m \leq r \leq 150\ \mu m$. The aerosol spectrum obtained for each 429-m path is designated n(r), and the average of the 15 spectra along the 6.44-km path is designated <n(r)>.

Figures 2 and 3 respectively present <w> and <A> obtained from <n(r)> at each flight level on M29 and A18 as a function of distance z* from the cloud base (defined as the level where $w = 0.02\ g/m^3$). Figure 4 presents examples of <n(r)> at selected levels on M29 and A18, and table 1 contains <w>, <A>, <N>, $<\bar{r}>$, and $<\sigma_r>$ for these <n(r)>s. Figure 5 presents <N(z*)> and $<\bar{r}(z^*)>$ for the <n(r)>s in and near the cloud.

---

†Aerosol spectrum units are $cm^{-3}\mu m^{-1}$.

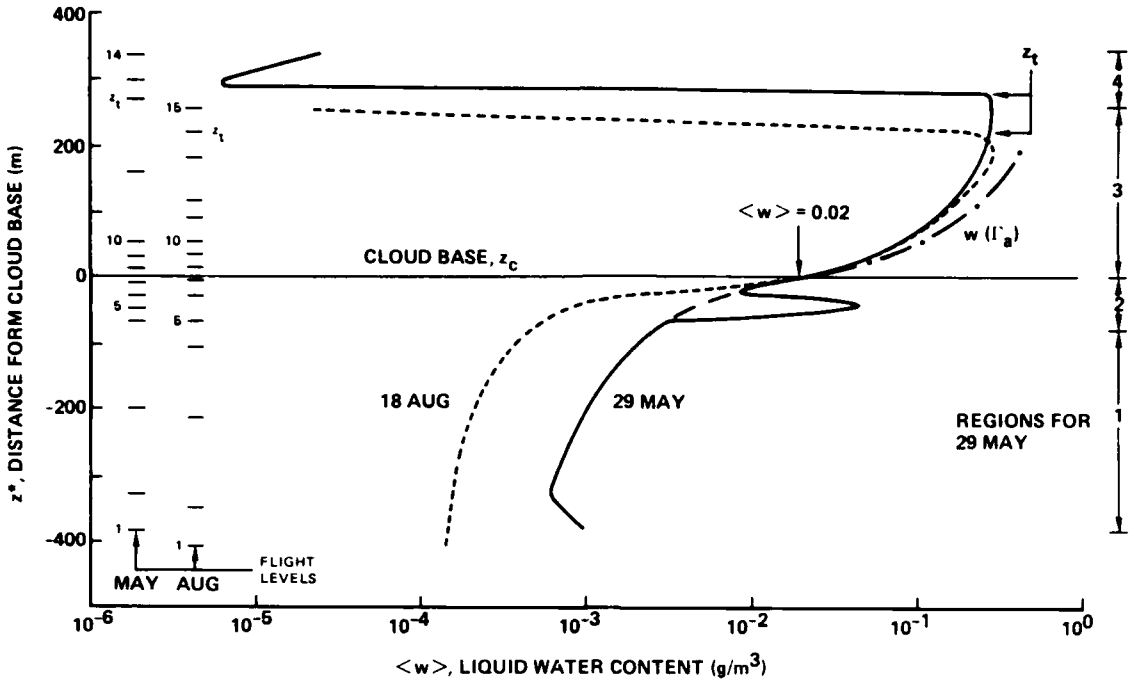

Figure 2. Profiles of the liquid water content, $< w >$, calculated from the aerosol spectrum (eq 4) representing 6.44-km horizontal runs at the indicated measurement levels on 29 May and 18 August. The zero reference level here and in figure 3 is cloud base, defined to be at the level where $< w >$ is 0.02 g/m^3.

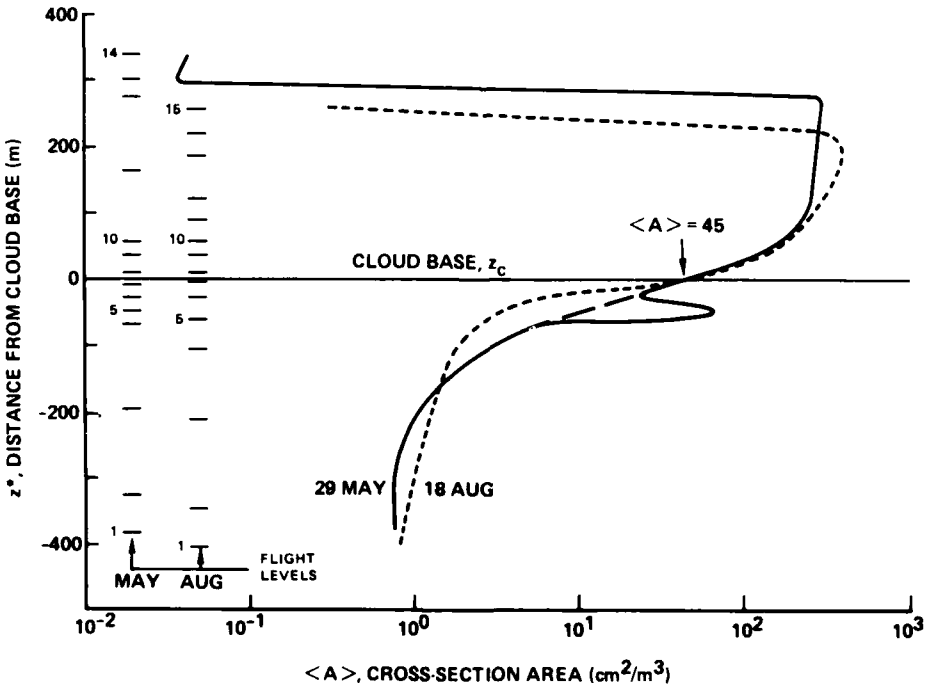

Figure 3. Profiles of the cross-section area, $< A >$, calculated from the aerosol spectrum (eq 3) representing 6.44-km horizontal runs at the indicated measurement levels on 29 May and 18 August.

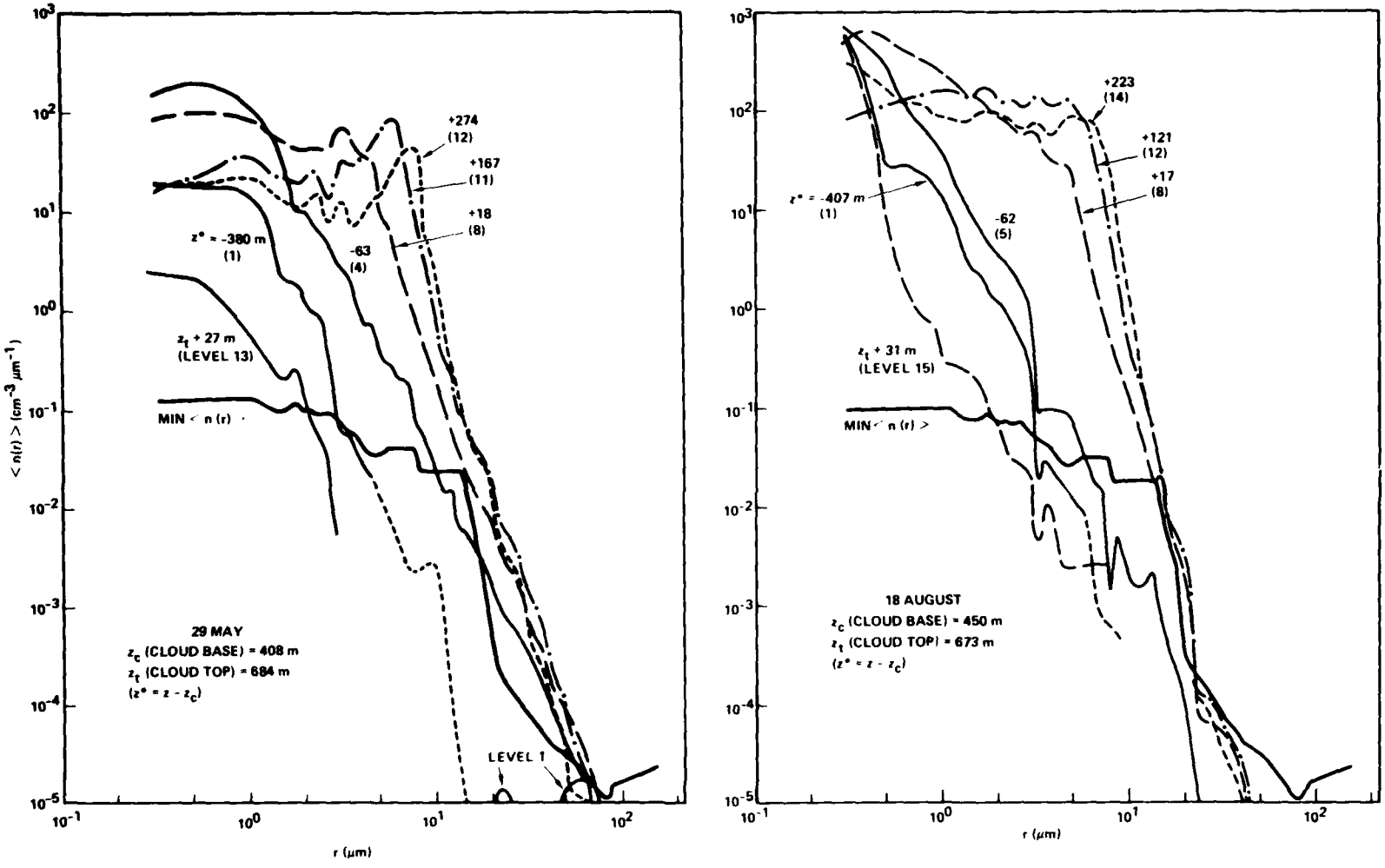

Figure 4. Aerosol spectra representing 6.44-km horizontal runs at selected distances (flight levels) from cloud base on 29 May and 18 August. Min <n(r)> is the minimum <n(r)> for a 6.44-km run capable of being observed in each of the 15 segments along the run when the aerosols in each radius band are distributed equally along the horizontal run.

Flight Level No	z^* (= $z-z_c$) (m)	From Avg n(r) at Flight Level $\langle w \rangle$ (g/m^3)	$\langle A \rangle$ (cm^2/m^3)	$\langle N \rangle$ (cm^{-3})	$\langle \bar{r} \rangle$ (μm)	$\langle \sigma_r \rangle$ (μm)	From n(r)s along Flight Level σ_w (g/m^3)	σ_A cm^2/m^3	σ_N (cm^{-3})	$\sigma_{\bar{r}}$ (μm)
29 May 81										
1	-380	1.03(-3)	0.74	21	0.87	0.62	1.36(-3)	0.17	3	0.02
4	- 63	3.14(-3)	6.21	194	0.83	0.59	1.62(-3)	3.51	71	0.11
8	18	3.37(-2)	52.6	260	2.00	1.57	2.19(-2)	31.7	43	0.66
11	167	2.17(-1)	257.0	296	4.82	2.09	2.90(-2)	33.2	31	0.22
12(z_t)	274	2.88(-1)	286.0	228	5.77	2.60	1.03(-1)	99.0	60	1.03
13	301	6.46(-6)	0.04	2	0.70	0.45	1.84(-6)	0.01	33	0.05
18 Aug 81										
1	- 407	1.35(-4)	0.89	111	0.41	0.29	3.68(-5)	0.24	65	0.11
5	- 62	5.41(-4)	2.50	213	0.49	0.36	1.40(-4)	0.61	71	0.07
8	17	3.74(-2)	72.7	589	1.48	1.32	3.93(-2)	70.3	148	0.79
12	121	1.99(-1)	292.0	693	3.13	1.91	6.00(-2)	74.7	40	0.43
14(z_t)	222	2.63(-1)	329.0	575	3.56	2.37	1.33(-1)	168.0	164	1.12
15	254	2.15(-5)	0.30	90	0.31	0.09	1.39(-5)	0.19	57	0.05

[v] **The numbers in parentheses are the powers of ten by which the preceding number must be multiplied.**

Table 1. Parameters derived from the average aerosol spectrum representing the 6.44-km horizontal runs and parameters derived from the 15 aerosol spectra taken along the runs (15 segments of 429 m each), at selected distances from the cloud base.

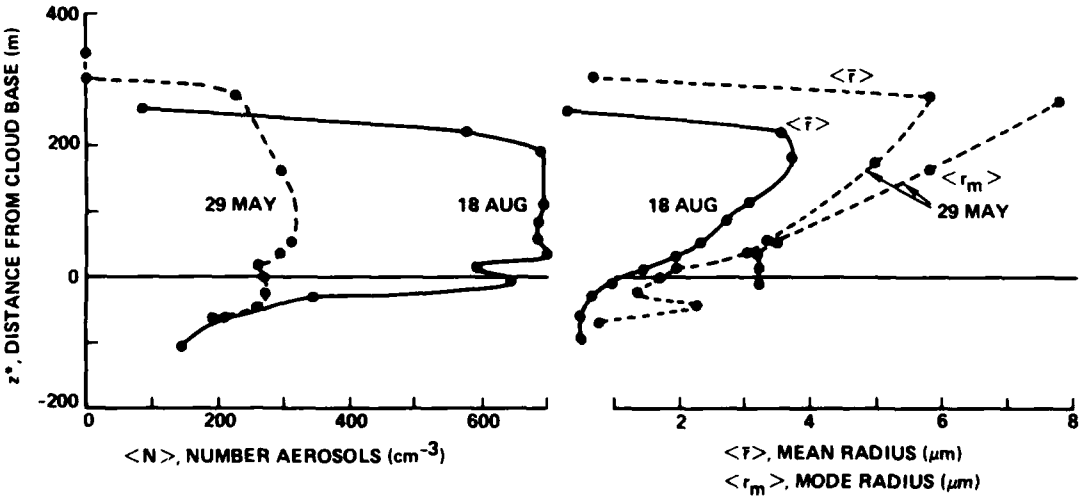

Figure 5. Profiles of parameters derived from the aerosol spectrum representing 6.44-km horizontal runs at flight levels in and near the clouds on 29 May and 18 August.

5. AIR MASS

a. COMPARISON OF <N>, $\langle\bar{r}\rangle$, AND $\langle\sigma_r\rangle$

The number of aerosols, <N>, was greater on A18 at all levels (fig 5 and table 1). <N> was about five times greater on A18 at level 1 and was about two times greater on A18 near midcloud (level 11 on M29, level 12 on A18). Midcloud values of <N> were 296 and 693 cm^{-3} respectively for M29 and A18. Pruppacher and Klett (1978) give examples in which $N \cong 220\ cm^{-3}$ in continental clouds and $N \cong 55\ cm^{-3}$ in marine clouds, at $r \gtrsim 3\ \mu m$. These Ns are about one-half and one-fourth of the observed <N>s for A18 and M29 respectively at $r \gtrsim 3\ \mu m$ near midcloud. Both $\langle\bar{r}\rangle$ and $\langle\sigma_r\rangle$ are larger at all elevations on M29. Pruppacher and Klett (1978) give examples showing that n(r)s in clouds are characterized by larger $\langle\bar{r}\rangle$s and $\langle\sigma_r\rangle$s for marine air masses. Accordingly, data on M29 might be considered to characterize a marine air mass, and data on A18 might be considered to characterize a continental air mass.

b. MODE IN <n(r)> ON 29 MAY

Curves b and c in figure 6 show the values of n(r)s measured in clouds by the same instrumented aircraft on 9 May 1978 near San Nicolas Island, California, when thin scattered stratus clouds were observed (Noonkester, 1981a). The presence of strong convective mixing during this time was indicated by radiosonde observations of the vertical temperature structure and tower measurements (from the NW tip of San Nicolas Island) of surface heat flux. The scattered clouds were 30 to 40 m thick. Air trajectory analysis and a low radon count indicated the presence of marine air.

Curve a in figure 6 shows <n(r)> at $z^* = 38$ m (level 9) on M29. Except for the region $r < 2\ \mu m$, <n(r)> on M29 is essentially identical to the n(r)s for the convective marine air on 9 May 1978. Neiburger and Chien (1960) observed an n(r) in a stratus-cloud layer almost identical to the n(r)s in figure 6. They provided an aerosol model capable of producing a strong mode ($r \cong 5$ to 9 μm) in the lower portion of a cloud formed by slow adiabatic cooling of air containing salt nuclei. Fitzgerald (1974) and Lee et al (1980) also developed models capable of producing a mode in clouds for nuclei approximating a marine air mass. (Figure 5 shows the radius, r_m, at the peak of the mode in <n(r)> for $r > 2\ \mu m$.) These data suggest that a marine air mass was present on M29.

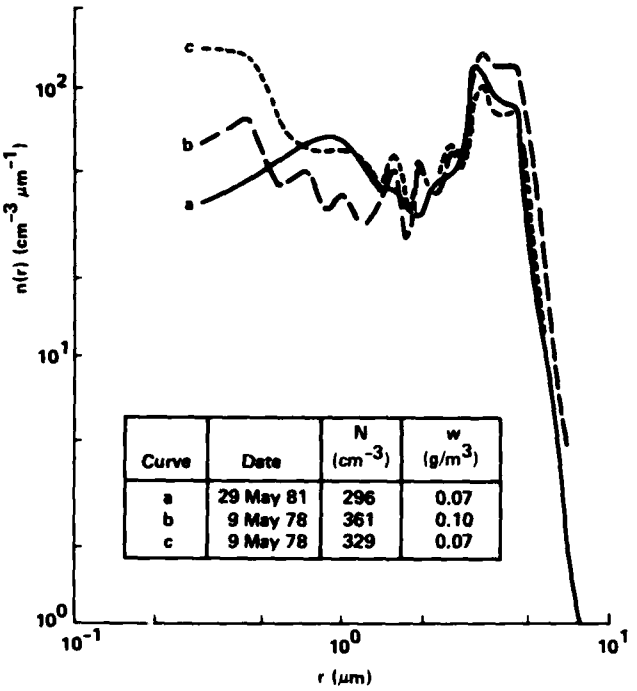

Figure 6. Aerosol spectra observed about 35 m above the base of marine stratus clouds on two separate days. Thin scattered stratus clouds were present in a convective layer capped by a subsidence inversion on 9 May 1978 (Noonkester, 1981a), whereas the cloud on 29 May 1981 was a widespread homogeneous deck.

c. SURFACE AIR FLOW

To estimate the air mass source at the measurement site, an average surface pressure pattern was constructed for a large region surrounding the measurement site shown in figure 1. The 0400 PST synoptic surface pressure maps given by facsimile copies of NOAA analyses were used. Synoptic maps on 13, 14, 27, 28, and 29 May 1982 were used to represent the measurement periods on 14, 28, and 29 May; and maps on 10, 11, 12, 13, 14, 16, 17, and 18 August were used to represent the measurement periods on 11, 13, 14, 17, and 18 August. Average pressures were determined for the intersections of all 5° lines of longitude and latitude shown in figure 1. The representative average surface pressure patterns for the measurement periods in May and August are shown in figure 1.

The average pressure pattern in August indicates that a continental air mass flow would be present in the measurement region even if the cross-isobaric flow out of the high-pressure region were large. The average pressure patterns for May and August are similar south of 40°N latitude along the California coast. Thus the pattern during May does not clearly reveal a marine air mass flow in the measurement region.

The east-west pressure gradient was greater during May, west of San Diego. A stronger cross-isobaric flow (more westerly wind) is expected in the San Diego region when the east-west pressure gradient increases. Observation of the ocean surface in the measurement region indicated a WNW surface wind on M29 and a NW surface wind on A18. The fact that the wind was more westerly at the measurement site on M29 supports the assumption that an overocean air-parcel trajectory existed upwind of the measurement site.

The above data provide good reason to conclude that a marine air mass was present on M29 and that a continental air mass was present on A18.

6. VERTICAL VARIATIONS OF <n(r)>

a. CLOUD BASE

Vertical changes of <n(r)> are expected to be a function of the distance from the level of saturation near the lower portion of the cloud rather than a function of the distance from the cloud top or surface. Thus, comparison of vertical changes of <n(r)> relative to the level of saturation is appropriate. The level of saturation could not be determined from the measurements. A reference level, based on the liquid water content, w (eq 4), and assumed to be near the level of saturation, was established to permit comparisons of the aerosol data on M29 and A18.

The bases of the stratus clouds were assumed to be at the level at which $\langle w \rangle = 0.02\ g/m^3$. Figure 2 shows <w> as a function of the distance z^* from the cloud base z_c, where $\langle w \rangle = 0.02\ g/m^3$, and shows the measurement levels relative to z^*. Figure 3 gives the cross-sectional area, A (eq 3), as a function of z^*. The profiles in figures 2 and 3 were drawn through all data points at elevations indicated by the flight levels. Except for unexplained large values of <w> and <A> at level 5 on M29, the <w>s and <A>s are well-behaved continuous functions of z^*.

The defined cloud base can be associated with horizontal visibility by using an optical extinction coefficient in the visible range along with Koschmieder's equation (Middleton, 1968). The optical extinction coefficient, k, at wavelength λ is as follows:

$$k = \pi \int Q_e\left(\frac{2\pi r}{\lambda}, m\right) r^2\, n(r)\, dr\ , \qquad (6)$$

where Q_e is the total scattering cross section calculated from Mie theory and normalized by geometric cross section, and m is the complex index of refraction. In the visible range $Q_e \cong 2$, so that

$$k \cong 2\pi \int r^2 n(r)\, dr$$
$$\cong 2A \quad . \tag{7}$$

According to Koschmieder, the meteorological visual range, v, is related to $k_e(\lambda \cong 0.5\ \mu m)$ as follows:

$$kv = 3.912 \quad . \tag{8}$$

Combination of (7) and (8) provides

$$v = \frac{3.912}{2A} \quad . \tag{9}$$

From figure 3, A = 4.5 km^{-1} at z_c, so that k (visible range) = 9.0 km^{-1} according to equation (7). Numerical integration of equation (6) for <n(r)> at level 7, just below z_c (fig 2), produces $k_e(\lambda = 0.53\ \mu m)$ values of 8.6 and 9.1 km^{-1} respectively for M29 and A18. These values are near 9.0 km^{-1}, as estimated from A (eq 7). Equation (9) yields a v of 435 m for k = 9 km^{-1}. According to the international visibility code, a visibility of 435 m would be observed in a moderate fog. Thus, the association of a <w> of 0.02 g/m^3 with a cloud base appears reasonable and serves to define cloud base in this report.

b. CHARACTERISTIC REGIONS OF <w(z*)> AND <A(z*)>

The vertical profile of <w> in figure 2 reveals four general regions of differing vertical gradients, categorized as follows:

Region 1: small exponential increase in the range -200 m < z* < -80 m
Region 2: moderate exponential increase in the range -80 m < z* < 0
Region 3: large linear increase in the range 0 < z* < (z_t - 40 m)
Region 4: large decrease in the region near z_t through an elevation difference of about 40 m.

These regions may roughly represent regions of different aerosol growth characteristics related to ranges of relative humidity, f. The dry adiabatic

gradient $\Delta f/\Delta z$ is about +1% per 20 m for conditions on M29 and A18 for f near 99 percent. If f is 100 percent at z_c, f $\cong$ 96% at z* = -80 m for dry adiabatic changes. Fitzgerald (1975) gives an aerosol growth rate factor providing a slow aerosol size growth rate for f $\tilde{<}$ 96% and a rapid increase in the aerosol growth rate for 96% $\tilde{<}$ f < 99.5%. Thus, transitions in $\Delta w/\Delta z$ and $\Delta A/\Delta z$ might be expected near z* = -80 m. In the cloud, supersaturation would produce activated aerosols and $\Delta w/\Delta z$ and $\Delta A/\Delta z$ would be large. The expected rapid decrease of f above z_t, with mixing across z_t, would produce the large decrease in <w> and <A> above z_t.

c. ANALYTICAL DESCRIPTION OF <w(z*)> AND <A(z*)>

The profiles of <w> and <A> (fig 2 and 3) are essentially linear above z_c in Region 3 if data at z_t are omitted. After omitting data at z_t, regression analysis of data for levels 8-11 on M29 and for levels 8-13 on A18 gives the following.

M29:
$$\langle w \rangle = 0.019 + 0.0012z^* \ (g/m^3) \quad (10)$$
$$\langle A \rangle = 50 + 1.3z^* \ (cm^2/m^3) \quad (11)$$

A18:
$$\langle w \rangle = 0.0074 + 0.0016z^* \ (g/m^3) \quad (12)$$
$$\langle A \rangle = 54 + 1.9z^* \ (cm^2/m^3) \ , \quad (13)$$

where z is in metres.* From equation (10), <w> is 0.26 g/m^3 at z* = 200 m. Observations in two nocturnal stratocumulus cloud layers over land by Slingo et al (1982) show w values of about 0.24 and 0.30 g/m^3 at z* = 200 m, in good agreement with data on M29.

In Region 2 the profiles of <w> and <A> are exponential. A regression analysis of data for levels 4-8 on M29 and for levels 5-8 on A18 gives the following.

M29:
$$\langle w \rangle = 0.019 \ e^{0.030z^*} \ (g/m^3) \quad (14)$$
$$\langle A \rangle = 38 \ e^{0.027z^*} \ (cm^2/m^3) \quad (15)$$

A18:
$$\langle w \rangle = 0.014 \ e^{0.059z^*} \ (g/m^3) \quad (16)$$
$$\langle A \rangle = 34 \ e^{0.045z^*} \ (cm^2/m^3) \ , \quad (17)$$

where z^* is in metres. The correlation coefficients for all the above regression equations are at least 0.98.

In contrast to $\langle w(z^*)\rangle$ in the cloud given by equations (10) and (12), the liquid water liberated by condensation in a moist adiabatic ascent is approximately as follows.

$$\text{M29:} \qquad w(\Gamma_a) \cong 0.0022z^* \ (g/m^3) \tag{18}$$

$$\text{A18:} \qquad w(\Gamma_a) \cong 0.0025z^* \ (g/m^3) \ , \tag{19}$$

where z^* is in metres. Figure 2 contains $w(\Gamma_a)$ for the average gradients of equations 18 and 19. The ratios of the observed to the adiabatic gradient of w are 0.55 for M29 and 0.64 for A18. These ratios are less than found by Schmetz et al (1981) in daytime maritime stratocumulus clouds and by Slingo et al (1982) in nocturnal stratocumulus clouds over land.

d. AEROSOL SPECTRA

Figure 4 presents $\langle n(r)\rangle$ at six measurement levels on M29 and A18. Table 1 contains $\langle w\rangle$, $\langle A\rangle$, $\langle N\rangle$, $\langle \bar{r}\rangle$, and $\langle \sigma_r\rangle$ for these spectra. Vertical changes in the aerosol spectra representing Regions 1, 2, 3, and 4 are only partially illustrated in figure 4. The vertical changes in $\langle n(r)\rangle$ might be expected as f increases with elevation until saturation is attained near z_c. Changes in Region 1, represented by levels 1 to 4 on M29 and levels 1 to 5 on A18, show an increase in $\langle n(r)\rangle$ that is greater on M29 at all values of r. Region 2, represented by levels 4 to 8 on M29 and levels 5 to 8 on A18, has a large increase in $\langle n(r)\rangle$ except at small r, particularly in the 2 to 5 μm radius size range. Region 3, represented by levels 8 to 11 on M29 and levels 8 to 12 on A18, has a large increase of $\langle n(r)\rangle$ in the 5 to 10 μm radius size range. The increase in $\langle \sigma_r\rangle$ in Region 3 demonstrates the spreading of the spectrum above the cloud base. Region 4, represented by levels 12 to 13 on M29 and levels 14 to 15 on A18, has an extremely large decrease in $\langle n(r)\rangle$ at all values of r except at $r < 0.5$ μm on A18.

In contrast to these similarities, the $\langle n(r)\rangle$s in figure 4 show four major differences: (1) $\langle n(r)\rangle$ is much greater at small values of r on A18 and is greater at large values of r on M29, at all elevations. (2) The increase of $\langle n(r)\rangle$ with elevation is greater on M29 in Region 1. (3) $\langle n(r)\rangle$ increases

more with elevation in Region 2 on A18. (4) A strong mode forms in <n(r)> on M29, while a plateau forms in <n(r)> near 10^2 cm^{-3} μm^{-1} on A18 in Region 3 for $r \lesssim 8$ μm.

Figure 5 depicts <N>, $\langle \bar{r} \rangle$, and $\langle r_m \rangle$ in Regions 2, 3, and 4. <N> is about 200 cm^{-3} at the bottom of Region 2 on M29 and A18, but increases to about 275 cm^{-3} on M29 and to about 600 cm^{-3} on A18 at the top of Region 2. The gradual increase of <n(r)> at large values of r in Region 3 is revealed by the increase in $\langle \bar{r} \rangle$. $\langle \bar{r} \rangle$ is greater on M29 because <n(r)> is greater at large values of r on M29. The modal radius $\langle r_m \rangle$ on M29 increases almost linearily from 3.2 to 7.8 μm from $z^* = 38$ m to z_t ($\Delta r_m/\Delta z = 1.9$ μm per 100 m). Slingo et al (1982) presented observations of two nocturnal stratocumulus clouds over land wherein N was about 250-300 cm^{-3} in midcloud and the ($\Delta r_m/\Delta z$) values were about 1.7 and 0.7 μm per 100 m. These two sets of data approximate data on M29.

7. SPECTRAL VARIABILITY ALONG FLIGHT LEVELS

a. AEROSOL SAMPLING

According to the discussion in appendix A, the horizontal variability of n(r) cannot be determined if the number of aerosols in any radius band is less than 15 for the OAP-200 and less than 60 for the ASSP-100, over the 6.44-km path. Figure 4 shows <n(r)> for these minimum particle counts, termed min <n(r)>. The <n(r)>s less than min <n(r)> cannot be observed in all 15 segments along the path but may be observed in some, when the aerosols are homogeneously distributed. The portions of the <n(r)>s much greater than min <n(r)> control <N> and $\langle \bar{r} \rangle$. The portions of the <n(r)>s about equal to or less than min <n(r)> sometimes control <w> and <A>. Thus horizontal variability can be determined without hesitation for N and $\bar{r}$ but not for w and A when the 15 n(r)s along the 6.44-km path are used. The data points circled in figure 7 are at levels where the number of aerosols along the 6.44-km path are too small to determine the horizontal variability.

b. HORIZONTAL VARIABILITY OF SPECTRAL PARAMETERS

Each n(r) for the fifteen 429-m segments was characterized by N, A, w, and $\bar{r}$. The ratio σ_x:<x> was used as a measure of variability along the path,

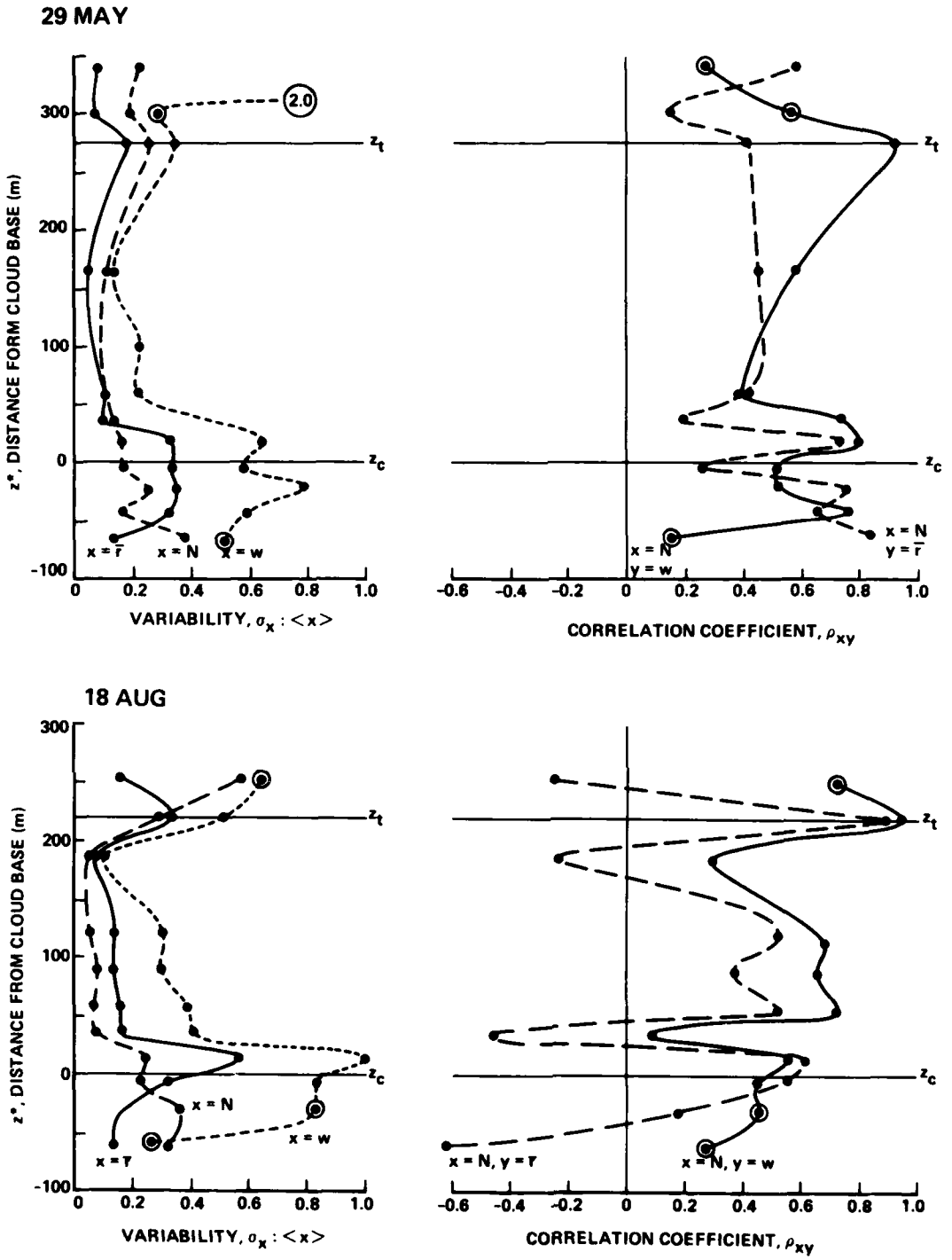

Figure 7. Profiles of the variability and correlation coefficient of aerosol parameters at measurement levels in and near the clouds on 29 May and 18 August. The parameters were calculated from the 15 aerosol spectra taken along the 6.44-km horizontal runs.

where x is N, A, w, or $\bar{r}$. σ_x is the standard deviation of x, and <x> indicates the average x over the 6.44-km path. The nature of the relative changes between two parameters along the path was represented by the linear correlation coefficient ρ for the pairs (N, w) and (N, $\bar{r}$). Figure 7 depicts σ_x:<x> and ρ at all measurement levels in and near the cloud. Because σ_A:<A> is almost identical to σ_w:<w> and because $\rho(A, w) \cong 1$, the statistics σ_A:<A> and $\rho(A, w)$ are not given in figure 7.

To estimate the average horizontal scale size, λ, of the parameter variations along each flight level, the number of positive and negative deviations, α, of an aerosol parameter from its average over the flight levels was obtained. The number of λs at a flight level is assumed to be 0.5α, so that $\lambda \cong 6.44(0.5\alpha)^{-1}$ km. The average α for all parameters at all levels shown in figure 7 was 3.5. Thus, the 6.44-km paths contained about 1.8 λs, and $\lambda \cong 3.7$ km. The maximum α was 5.1 for N and the minimum α was 2.6 for A. The average standard deviation of α was 1, giving a 2σ range of λ from 2.9 to 5.2 km. Accordingly, because appreciable trends ($\lambda > 6.44$ km) are not present, consecutive sampling distances of 429 m over the 6.44-km path appear adequate to obtain statistics of aerosol parameters.

The major features of σ_x:<x> in figure 7 are a primary maximum around z_c, a secondary maximum near z_t, and a minimum in the cloud. Vertical turbulent mixing is believed to be the most likely cause of the horizontal variability, because the average gradient of the relative humidity, f,—the principal controlling factor of n(r)—is greater in the vertical plane than in the horizontal plane. Vertical motion of aerosols across the level where $f \cong 100\%$ near z_c and z_t is expected to create large changes in n(r) compared to changes associated with vertical motion within the cloud. The proposed source of variability is highly tentative, in the absence of knowledge on the simultaneous variations of n(r) and f along the trajectory of the air parcel carrying the aerosols with entrainment at z_t included.

c. HORIZONTAL CORRELATIONS OF SPECTRAL PARAMETERS

Vertical changes in ρ for the pairs of parameters (N, w) and (N, $\bar{r}$) along the flight levels presented in figure 7 appear to have few significant features. $\rho(N, w)$ is positive at all levels and approaches 1 at z_t on M29 and A18. $\rho(N, \bar{r})$ is positive at all levels on M29 but is negative at four levels

on A18. A $\rho > 0.5$ is significant at the 5 percent level. All but one ρ for (N, w) are significant at the 5 percent level on M29 and all but three ρs are significant on A18.

A positive correlation between N and w indicates that an increase of n(r) in the spectral region controlling the increase in w is proportional to the total increase of N, but n(r) may decrease in some ranges of r. Similarly, a positive correlation between N and $\bar{r}$ indicates that an increase of n(r) in the spectral region controlling the increase in $\bar{r}$ is proportional to the total increase in N, but n(r) may decrease in some ranges of r. Thus, these correlations cannot reveal the changes in n(r) over the entire range of r as N, w, and $\bar{r}$ change. If n(r) were assumed to increase over the entire spectrum when N increases, then N and w would be positively correlated. But when N increases in observed spectra, $\bar{r}$ can increase or decrease depending on the radius regions having the largest relative increase in n(r), and the correlation, $\rho(N, \bar{r})$, can be either positive or negative. Data of $\rho(N, \bar{r})$ and ρ(N, w) on M29 show that both w and $\bar{r}$ consistently increase as N increases at all levels.

8. DISCUSSION

a. CLOUD BASE

Because vertical variations of $\langle n(r) \rangle$ characteristics are the major considerations in this report, the definition of cloud base, the reference level, is an important issue.

The presence of a horizontally extensive marine stratus-cloud layer capped by a subsidence inversion near the surface of the ocean is generally concluded to indicate the presence of a well-mixed boundary layer where the vertical temperature gradient below the cloud approaches a dry-adiabatic rate and the gradient in the cloud approaches, but is less than, a moist-adiabatic rate. The region where the relative humidity, f, is 100 percent separates the distinctly different temperature lapse rates. Relative to the vertical changes in the aerosol spectrum $\langle n(r) \rangle$, the most significant changes occur near the level where f is 100 percent. Vertical changes in characteristic features of $\langle n(r) \rangle$ are expected by theory, have been observed to be different above and below the saturation level, and are related to changes in the

dominating physical processes controlling aerosol growth. The enhanced condensation of water vapor onto the aerosols and the release of latent heat change the temperature lapse rate above the saturation level. Thus when the vertical changes in $\langle n(r) \rangle$ in marine stratus-cloud layers are compared, the level of saturation is a realistic reference level.

The level of saturation could not be identified during the measurements. Observations aboard airborne platforms in marine stratus layers show that the vertical transition from a cloudfree (good visibility) to a cloudy (poor visibility) atmosphere is gradual; a cloud base or effective saturation level cannot be visually identified.

For many purposes optical properties are the most significant features of clouds and can be used to identify their presence just as horizontal visibility is used to identify the presence of fog. When the optical extinction coefficient, k (eq 7), and the liquid water content, w (eq 4), are calculated from the observed n(r), the linear correlation coefficients between k and w are greater than 0.98, given 0.53 to 10.59 μm optical wave lengths, Λ, and the following relation (Hughes and Jensen, 1978; Noonkester, 1981b), where regression analysis is used to obtain a and b:

$$k = aw^b \quad . \tag{20}$$

Thus by defining the base of stratus clouds to be at the level where $\langle w \rangle = 0.02$ g/m^3, the associated optical extinction coefficients for a large range of Λs can be obtained. For $\Lambda = 0.53$ μm, the visibility is about 435 m when $\langle w \rangle = 0.02$ g/m^3 for these data.

Section 6 shows that the vertical gradients of $\langle w \rangle$ and $\langle A \rangle$ change from exponential to linear near the level where $\langle w \rangle = 0.02$ g/m^3, the cloud base (para f). This suggests that the defined cloud base may be near the level of saturation. Although the selection of $\langle w \rangle = 0.02$ g/m^3 to identify cloud base is arbitrary, an appreciable increase (+0.03 g/m^3 for +20 m) or decrease (-0.01 g/m^3 for -20 m) in the value of $\langle w \rangle$ for the cloud base would place the cloud base at a level where the visibility (respectively 200 m and 800 m for ±20-m change in z_c) might not be generally accepted as appropriate for the presence of a cloud.

b. **AEROSOL SPECTROMETERS**

The differences between measured and true n(r)s are unknown. Some inherent problems with the aerosol spectrometers used in the measurements have been examined by several investigators (eg, Slingo et al, 1982) and cannot be avoided. Careful use, including regular calibrations, should have reduced some errors (such as the sampling volume) and greatly increased the repeatability of the sensors. Comparisons of data taken by sensors used here with data taken by others with similar sensors in stratus clouds indicate a high level of repeatability; that is, the sensors were considered capable of providing reliable relative changes in n(r) for measurements separated in time and position.

c. **SAMPLING TIME FOR LAYER**

The total sampling time for the stratus layers was dictated by a compromise between the number of sample levels and the horizontal distance (sampling volume) judged necessary to obtain a representative $\langle n(r) \rangle$. The stratus layers were considered to be in a near steady-state condition during the time (~ 1 h) required to make the measurements. Measurements at night, when temporal changes might be minimal, could not be made because good visibility is required along low-level flights, to avoid surface vessels. Early morning measurements (0610 to 0904 PST) were made to reduce possible changes induced by solar heating, which is likely to be a maximum near 1200 PST.

d. **SAMPLING DISTANCE AND HORIZONTAL VARIABILITY**

According to Lumely and Panofsky (1964), a horizontal averaging distance, L, necessary to obtain acceptable averages of $\langle x \rangle$ is a function of the population (or ensemble) variability, $\sigma_x : \langle x \rangle$, the acceptable level of error, ε, and an integral scale length, ℓ_x, where

$$L \sim 2\ell_x \left(\frac{\sigma_x : \langle x \rangle}{\varepsilon} \right)^2 \quad . \tag{21}$$

In a mixed layer, ℓ_x scales with the depth of the mixed layer z_t. The sample variability, $\sigma_x : \langle x \rangle$, is used as an estimate of the population variability. If $(\sigma_x : \langle x \rangle)\varepsilon^{-1}$ were unity, L would equal about 2 ℓ_x (1.3 km) on M29 and A18, and

the 6.44-km runs would have provided acceptable averages of <x>. But for an ε of 10 percent, the average $(\sigma_x : \langle x \rangle)\varepsilon^{-1}$ was much greater than unity and the average L was 30 km, which is 4.7 times greater than 6.44 km.

Table 2 gives L for <w>, <A>, <N>, and $\langle \bar{r} \rangle$ at eight levels on M29 and seven levels on A18 when a 10 percent error (ε) in the averages is acceptable. Some values of $\sigma_x : \langle x \rangle$ used to calculate L in table 2 are shown in figure 7. L varies considerably with x and z^*, and the dependence of L on x and z^* is different on M29 and A18. The largest average L occurs at z_t + 68 m (z^* = 343 m) on M29 and at z^* = 17 m on A18; the smallest average L occurs near midcloud on both days. <w> on M29 requires the largest average L, and $\langle \bar{r} \rangle$ on M29 requires the smallest average L. At z_t + 69 m on M29, L ranges from the maximum of 528 km for <w> to 1.0 km for $\langle \bar{r} \rangle$. Although <w> and <A> appear to be excessively large at level 5 on M29 (fig 2 and 3), values of L at level 5 in table 2 for M29 do not suggest unusual conditions.

Flight Level No	z^* (= $z-z_c$) (m)	L (km) <w>	<A>	<N>	$\langle \bar{r} \rangle$	Avg
29 May 81						
3	-189	163	11	4.5	0.2	45
4	-63	38	44	18	2.7	26
5	-40	48	52	3.5	15	30
8	18	58	50	3.7	15	32
11	167	2.4	2.3	1.5	0.3	1.6
12(z_t)	274	18	16	9.5	4.5	12
13	301	11	7.8	5.2	0.8	6.2
14	343	528	23	6.9	1.0	140
Avg		108	26	6.6	4.9	37
18 Aug 81						
3	-209	5.0	1.7	11	4.4	5.5
5	-62	9.0	8.0	15	2.4	8.6
8	17	149	126	8.5	45	82
12	121	12	8.8	0.4	2.7	6.0
13	188	1.3	1.0	0.3	0.6	0.8
14(z_t)	222	34	15	11	16	19
15	254	56	55	46	3.6	40
Avg		38	31	13	11	23

Table 2. Approximate horizontal flight distance, L (eq 21), required to obtain estimates of the average aerosol spectrum parameters with a 10 percent error.

These estimates of L are independent of the variability (σ_x:<x>) sources, which could be instrumental, in the sampling technique, in digitization or data processing, or atmospheric. Digitization and data processing were concluded to have introduced negligible variations. The variability (σ_x:<x>) is largest near z_c and z_t and is the least in midcloud. There is no reason to believe that the instrument and sampling technique would create a minimum variability in the midcloud and a maximum near z_c and z_t. When <N> was greater than about 200 cm^{-3} (between $z^* = -60$ m and z_t), the number of aerosols appears to be adequate at radius bands controlling w, A, N, and $\bar{r}$. Thus neither instrumentation nor the sampling technique should introduce appreciable errors. If the variability could be reduced by, say, 25 percent, the average L would remain large at 23 km when ε is 10 percent. When L is 6.44 km and σ_x:<x> has a moderate value of 0.5 (fig 7), ε has the large value of 22 percent.

If values of L are known at all levels in the mixed stratus layer for all parameters derived from <n(r)>, an improved airborne measurement scheme can be devised. About 2.5 hours would be required to measure <n(r)> at 14 levels for an L of 30 km and an aircraft speed of 53.64 m/s (120 mph). The 30-km runs would likely include horizontal variability in the mesoscale region. If near-real-time data processing were available aboard the aircraft, realistic values of L could be estimated during the measurements. Otherwise, a priori values of L are required. Some mesoscale variability could be avoided by flying closed courses (circular, triangular, etc) at each level, but appreciable changes in the meteorological pattern could occur in a 2.5-hour measurement period. Reduction of L does not appear likely with existing aerosol sensing systems. Apparently, methods must be devised to increase the sampling volume rate and to decrease the sample variability created by sequential radius-band measurements such as used in the ASSP-100, particularly near the cloud top and base.

If the horizontal variations were caused by convective cells characterized by a λ of 3.7 km, the associated low-level instability could be estimated from results by Fitzjarrald (1978). Through the use of GATE data he found that $\lambda/z_t = 8.83(-z_t/L)^{-0.38}$, where L is the Monin-Obukhov length and $2.5 \lesssim -z_t/L \lesssim 60$. For the average z_t of 679 m on M29 and A18, his relation predicts a $-z_t/L$ of 3.6. Small values of $-z_t/L$ such as this are associated with weak instabilities, as might be expected in stratus-cloud layers. In

contrast, a $-z_t/L$ of 10 was observed in a moderate convective layer on 9 May 1978, when thin scattered stratus clouds were forming as described in section 5b. However, relationships between aerosol parameters and other variables like virtual temperature and vertical air motion must be determined before horizontal variations of aerosol parameters can be associated with convective cells.

e. PERTURBATION ON 29 MAY

Values of $\langle w \rangle$, $\langle A \rangle$, and $\langle \bar{r} \rangle$ at level 5 ($z^* = -40$ m) on M29 were appreciably larger than their corresponding values at levels 4 and 6 ($z^* = -61$ and -20 m respectively) and do not appear to be included in an exponential increase indicated by data at levels 4, 6, 7, and 8. Since a cloud is assumed to be present for $\langle w \rangle \geq 0.02$ g/m^3, a thin region near level 5 would be considered a cloud. However, data at level 5 were not considered to represent a well-mixed stratus layer, primarily because the data departed from an exponential increase, a reasonable expectation for aerosols in equilibrium as f approaches 100 percent. However, the data at level 5 on M29 are valid and appear to reveal a real perturbation. Similar perturbations were observed in other stratus-cloud data not presented here. Such perturbations must be examined as manifestations of important stratus-cloud physics, but data acquired in this study are inadequate to identify the physical process controlling the perturbation.

f. AVERAGE PROFILE OF $\langle w \rangle$

An average vertical profile, $\langle w(z^*) \rangle$, was obtained for the eight days of stratus data acquired in May and August and is shown in figure 8. These data were inadequate to extend the profile above $z^* = 250$ m, because the average cloud depth was 294 m and data near z_t were not used. The dashed line between $z^* = -20$ and -60m shows $\langle w(z^*) \rangle$ after eliminating the large perturbation at level 5 on M29.

The profile of $\langle w \rangle$ in figure 8 is a smooth-varying function of z^* with three relatively distinct regions identified as regions A, B, and C, corresponding to regions 1, 2, and 3 in figure 2. Analytical expressions for $\langle w(z^*) \rangle$, given in figure 8 for each region, were determined from least-square regression techniques; the correlation coefficients for the regression equations are greater than 0.98. The transition at $z^* = -250$ m may not be real, because runs near $z_c/2$ were minimal. For an adiabatic lapse rate of f,

f is about 96 percent at $z^* = -60$ m and about 83 percent at $z^* = -250$ m, under the assumption that f is 100 percent at cloud base. As indicated in section 6b, the rate of aerosol growth is expected to increase greatly when $f \gtrsim 96\%$. Thus the rapid increase of w above $z^* = -60$ m may be expected. The linear increase of $\langle w \rangle$ with z^* in the cloud at a rate less than the increase for a moist adiabatic lapse rate was expected.

The three days for May and the five days in August are considered to exhibit marine and continental air masses, and the average $\langle w(z^*) \rangle$ for May and August differed in the sense shown in figure 2. However, the differences between the May and August $\langle w(z^*) \rangle$s were less than a factor of 3 below z_c and were much less than the differences shown in figure 2. Thus figure 8 may manifest a coastal stratus layer when differences up to a factor of 3 are not important.

The data in figure 8 appear to show the first internally consistent vertical profile of w in the region ±250 m from cloud base representing a coastal marine stratus-cloud layer.

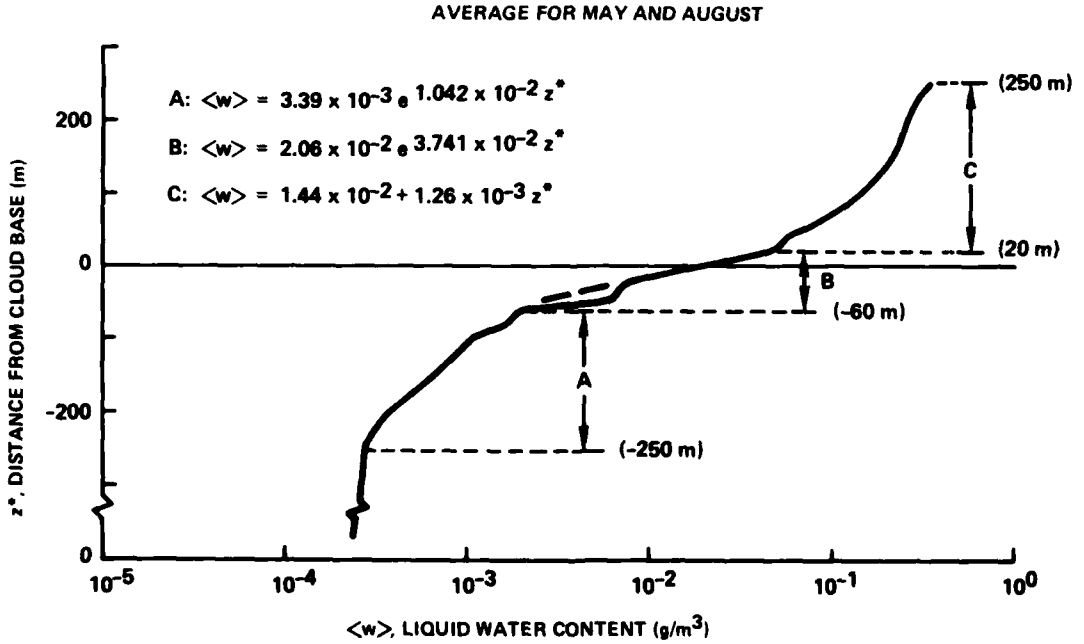

Figure 8. Profile of the average $\langle w \rangle$ for three stratus clouds in May (marine air mass) and five stratus clouds in August (continental air mass), with the May and August days equally weighted. The cloud base is at the level where $\langle w \rangle = 0.02$ g/m^3.

g. VARIATIONS IN SPECTRAL SHAPE

If spectral shape were conserved along the horizontal runs in the clouds, $\rho(N, \bar{r})$ would be about 0 and $\rho(N, w)$ would be about 1. Data in figure 7 do not show this trend at any level in the cloud. Inhomogeneous mixing (Latham and Reed, 1977), characterized by conservation of spectral shape, is apparently not present in the data presented here; although Slingo et al (1982) discussed data for nocturnal stratocumulus clouds over land, apparently supporting the presence of inhomogeneous mixing. Spectra found along some horizontal runs reveal highly similar spectral shape, but the test using $\rho(N, \bar{r})$ and $\rho(N, w)$ fails to support the presence of inhomogeneous mixing.

h. SPECTRAL FLATTENING AT SMALL r IN CLOUD

All $\langle n(r) \rangle$s showed a continuous reduction of $\langle n(r) \rangle$ at $r \lesssim 1.5$ μm as z^* increased above the cloud base, as shown for some elevations in figure 4. This decrease would not be expected if a large number of cloud condensation nuclei (CCN) were present and their radii increased sufficiently in the supersaturated cloud to move into the radius range ($r \geq 0.23$ μm) of the ASSP-100. The decrease of n(r) at small r suggests that the number of CCN capable of growing to $r \geq 0.23$ μm is minimal. A shortage of CCN would not be expected, as indicated by results of Hudson (1980) and Goodman (1977), in coastal marine fogs.

9. SUMMARY AND CONCLUSIONS

This report presents details on the changes in the aerosol spectrum n(r) from near the surface to the top of stratus-capped coastal marine layers in air masses considered to represent marine and continental air masses. The data are thought to be the first to show a smooth transition of aerosol spectral parameters over a depth from 250 m below to 250 m above the cloud base. These data differ from previous data in that they are internally consistent and show great detail near cloud base, defined as the level where $\langle w \rangle = 0.02$ g/m^3. The average $\langle w \rangle$, determined as a function of distance from cloud base z^*, shows three regions of characteristic changes in w apparently related to aerosol growth rates for three ranges of relative humidity. The $\langle n(r) \rangle$s showed a strong mode in the marine-air-mass clouds, while a plateau formed at small radii in the continental clouds. Although the values of w

were about the same in the clouds, more liquid water was contained in the small aerosols in the continental air mass than in the marine air mass.

Independent measurements were not available with which to determine the reliability of the aerosol measurements. Nevertheless, the data are thought to represent characteristic changes relative to the defined cloud base and are consistent with cloud data observed by others.

The finding that horizontal variability of n(r) was greater near the cloud base and cloud top might be expected with vertical mixing across regions where f is 100 percent. Horizontal changes of the spectral shape in the cloud do not support inhomogenous mixing.

According to the observed horizontal variability of the spectral parameters and theoretical averaging times required to obtain an acceptable average (Lumely and Panofsky, 1964), horizontal runs up to at least 30 km would be required to obtain averages of spectral parameters with a 10 percent error. This is 4.7 times greater than the run distance used. But if the May and August data are collectively considered to represent measurements in characteristic stratus-cloud mixed layers, the effective horizontal runs might be considered to be greater than 30 km and the averages would be more reliable. The profile of <w> for all days combined (fig 8) is believed to represent closely the relative vertical changes in a marine stratus layer.

The persistent use of the same measurement plan each day permitted great versatility in the data analysis. A similar approach is recommended for future overocean stratus cloud measurements.

REFERENCES

Baker MB, RG Corbin, and J Latham, 1980, The Influence of Entrainment on the Evolution of Cloud Droplet Spectra: I. A Model of Inhomogeneous Mixing, Quart J Roy Meteor Soc, vol 106, p 581-598.

Brost RA, DH Lenschow, and JC Wyngaard, 1982a, Marine Stratocumulus Layers—Part I: Mean Conditions, J Atmos Sci, vol 39, p 800-817.

Brost RA, JC Wyngaard, and DH Lenchow, 1982b, Marine Stratocumulus Layers—Part II: Turbulent Budgets, J Atmos Sci, vol 39, p 818-836.

Deardorff JW, 1980, Stratocumulus-Capped Mixed Layers Derived from a Three-Dimensional Model, Boundary-Layer Meteor, vol 18, p 495-527.

Fitzgerald JW, 1974, Effect of Aerosol Composition on Cloud Droplet Size Distribution: A Numerical Study, J Atmos Sci, vol 31, p 1358-1367.

Fitzgerald JW, 1975, Approximation Formulas for the Equilibrium Size of an Aerosol Particle as a Function of its Dry Size and Composition and the Ambient Relative Humidity, J Appl Meteor, vol 14, p 1044-1049.

Fitzjarrald DE, 1978, Horizontal Scales of Motion in Atmospheric Free Convection Observed During the GATE Experiment, J Appl Meteor, vol 17, p 213-221.

Goodman J, 1977, The Microstructure of California Coastal Fog and Stratus, J Appl Meteor, vol 16, p 1056-1067.

Hudson JG, 1980, Relationship Between Fog Condensation Nuclei and Fog Microstructure, J Atmos Sci, vol 37, p 1854-1867.

Hughes HG and DR Jensen, 1978, Extinction of IR Wavelengths by Aerosols in Coastal Fogs, Appl Optics, vol 17, p 2138-2140.

Jensen DR, R Jeck, G Trusty, and G Schacher, 1983, Intercomparison of PMS Particle Size Spectrometers, submitted to Optical Engineering.

Latham J and RL Reed, 1977, Laboratory Studies of the Effects of Mixing on the *Evolution of Cloud Droplet Spectra*, *Quart J Roy Meteor Soc*, vol 103, p 297-306.

Lee IY, G Hanel, and HR Pruppacher, 1980, A Numerical Determination of the Evolution of Cloud Drop Spectra due to Condensation on Natural Aerosol Particles, J Atmos Sci, vol 37, p 1839-1853.

Lumely JL and HA Panofsky, 1964, The Structure of Atmospheric Turbulence, John Wiley and Sons Inc.

Middleton WEK, 1968, Vision Through the Atmosphere, Un of Toronto Press.

Neiburger M and CW Chien, 1960, Computations of the Growth of Cloud Drops by Condensation Using an Electronic Digital Computer, Physics of Precipitation, Geophys Monograph 5 (NAS-NRC Pub 746), Am Geophys Union, p 191-210.

Noonkester VR, 1981a, Aerosol Size Spectra in a Convective Marine Layer with Stratus, Results of Airborne Measurements Near San Nicolas Island, California, J Appl Meteor, vol 20, p 1976-1980.

Noonkester VR, 1981b, Extinction Coefficients Calculated from Aerosol Spectra Measured in a Convective Layer with Stratus, Appl Optics, vol 20, p 1275-1277.

Pruppacher HS and JD Klett, 1978, Microphysics of Clouds and Precipitation, D Reidel Publishing Co.

Roach WT, R Brown, SJ Caughey, BA Crease, and A Slingo, 1982, A Field Study of Nocturnal Stratocumulus: I. Mean Structure and Budgets, Quart J Roy Meteor Soc, vol 108, p 103-123.

Schmetz J, E Raschke, and H Fimpel, 1981, Solar and Thermal Radiation in Maritime Stratocumulus Clouds, Beitr Phys Atmosph, vol 54, p 442-452.

Schubert WH, JS Wakefield, EJ Steiner, and SK Cox, 1979, Marine Stratocumulus Convection, Part I: Governing Equations and Horizontally Homogeneous Solutions, J Atmos Sci, vol 36, p 1286-1307.

Slingo A, R Brown, and CL Wrench, 1982, A Field Study of Nocturnal Stratocumulus: III. High Resolution Radiative and Microphysical Observations, Quart J Roy Meteor Soc, vol 108, p 145-165.

Telford JW and SK Chai, 1980, A New Aspect of Condensation Theory, Pure and Appl Geophys, vol 118, p 720-742.

APPENDIX A

AEROSOL PARTICLE COUNT

Each aerosol spectrum, n(r), was calculated from the relation

$$n(r) = \frac{PC(r)}{A(r)d\ B(r)}\ , \qquad (1A)$$

where

PC ≡ particle count

A ≡ sampling cross section of instrument

d ≡ sampling distance: (flight speed, V) × (flight time, t)

B ≡ bandwidth.

PC, A, and B are functions of the central radius, r, of the band. The spectrometers count the number of particles, PC, passing through the optical beam of the sampling area, A, over the distance, d, for each radius band, centered at r. The aircraft speed, V, was 53.64 m/s (120 mph). For the OAP-200, function A varies with r but is constant with time; while for the ASSP-100, A is constant at all values of r but varies slightly with time. The sampled volume is A × d. B is fixed for each probe.

The observed n(r) had to be given special attention for the purpose of determining horizontal variability when PC was small, a common condition outside the cloud.

All radius bands of the OAP-200 were sampled during the entire 8-s period. The total radius range of the ASSP-100 was sampled by sequentially sampling 4 subradius ranges for 2 s each, giving a complete n(r) for the ASSP-100 every 8 s. Thus for the OAP-200, all radius bands were sampled during each 8-s period; while for the ASSP-100, each radius band was sampled for 2 s each during each 8-s period. Each probe had a 0.4-s off time during the 8-s period, for electronic housekeeping and data storage. Although the 5 percent off-time was incorporated into calculating n(r), the off time is not considered here.

An n(r) (429-m path) calculated for the ASSP-100 can have a large error, particularly when the true PC = 1, 2, or 3 over the 8-s paths. When a certain number of particles is observed in a radius band within a 2-s observation

time window, n(r) is calculated by assuming that this number of particles would be observed during each of the three remaining 2-s periods (a homogeneous distribution). Let us assume a condition where aerosols are distributed randomly (but essentially homogeneously along the 8-s path) and no more than one aerosol is present in any 2-s path. When PC = 1 over the 8-s path and the particle is observed in a 2-s path, n(r) is calculated by assuming that PC = 4 over the entire 8-s path; this will occur 25% of the time. For true PC values of 2, 3, and 4, the corresponding percentages are respectively 50, 75, and 100 percent. A true n(r) can be obtained with the ASSP-100 only when the true PC is a multiple of 4 and the aerosols are distributed homogeneously. No assumption about horizontal homogeneity is necessary for the OAP-200, because all radius bands are sampled for the entire 8-s path although all aerosols of some radius bands may be closely grouped in a small portion of the path. The n(r)s and the $\langle n(r) \rangle$ will be the same if the aerosols are distributed homogeneously along the 6.44-km path and PC is a multiple of 15 for the OAP-200 and a multiple of 60 for the ASSP-100.


ATE
LME